

# SUBCRITICAL CRACK GROWTH OF WESGO AI-995 ALUMINA AT 1000°C

P.W. BACH

This report contains the results of subcritical crack growth experiments on Wesgo Al-995 alumina. This work has been performed in the framework of the project "Advanced Ceramics Testing and Design", nr. 6061.

CONTENTS

	<u>Page</u>
ABSTRACT	5
1. INTRODUCTION	6
2. EXPERIMENTAL PROCEDURE	8
2.1. Material	8
2.2. Time-to-fracture measurements	8
3. RESULTS AND DISCUSSION	10
4. CONCLUSIONS AND RECOMMENDATIONS	15
5. ACKNOWLEDGEMENTS	16
6. REFERENCES	17
TABLES	18
FIGURES	19



ABSTRACT

For the evaluation of ceramic components subjected to (thermo-)mechanical stresses, it is important to know the subcritical crack growth behaviour of the material. At ECN, research is directed to the development of ceramic components fabricated with strong fine grained ceramics. Subcritical crack growth can restrict the application of ceramics to rather low stress levels if it is not properly designed.

In the present investigation subcritical crack growth experiments in a 4-point bending device were performed on a commercial alumina Wesgo Al-995 at 1000°C. The subcritical crack growth parameters of Wesgo Al-995 alumina were determined with the modified lifetime method. The crack growth data points show a rather small scatter band around the fit line, which means that the data can be described by a simple power law. Within the experimental conditions there is no indication of a threshold at the lower end of the crack growth curve.

It is recommended to repeat these experiments with a larger serie of specimens (at least 20) and at several temperatures (600-1200°C) in order to obtain a better determination of the subcritical crack growth parameters of Wesgo Al-995 alumina.

## 1. INTRODUCTION

The objective of the IOP-TK project "Advanced Ceramics Testing and Design" is to develop and validate experimental and numerical methods for the failure probability and lifetime prediction of ceramic components. For the evaluation of ceramic components subjected to (thermo-)mechanical stresses, it is important to know the degradation behaviour of the material. The most important failure modes are:

- fast fracture
- subcritical crack growth
- creep
- cyclic fatigue
- corrosion.

Often a combination of these failure modes is involved in the degradation of ceramic components. Subcritical crack growth can cause catastrophic failure within the economic lifetime of a (thermo-)mechanical loaded ceramic component if it is not properly designed. Dependent on the type of ceramic, subcritical crack growth can occur at low and high temperatures in a non-vacuum environment. Alumina is especially prone to subcritical crack growth in a humid environment. The sensitivity of a ceramic material to subcritical crack growth can restrict the application of a ceramic component to rather low stress levels.

In fig. 1.1 a general type of subcritical crack growth curve is depicted with the crack growth rate versus the stress intensity  $K$ . To allow correct lifetime predictions the subcritical crack growth data or the power law relation parameters have to be known. Different methods for determining the data are available such as the double torsion method, the double cantilever beam technique, the dynamic bending method and the lifetime method. The first two, which were widely used in the past, are carried out with artificial macroscopic cracks (several millimeters), but in the latter two methods the crack growth of natural cracks is investigated. It is known that the lifetimes of components

cannot be predicted satisfactorily from the data obtained from specimens with large artificial cracks, especially for materials with a strong R-curve effect. It was observed that the growth rate can be more than 2 decades lower and the exponent of the power law relation by a factor of the order of 4 lower for natural cracks compared with macrocracks of several millimeters [7]. Also the macrocrack methods are usually restricted to relatively high crack growth rates, which are not characteristic for lifetime predictions of components. The lifetime method offers the possibility to investigate the subcritical crack growth behaviour of the naturally present defects in a ceramic over a large number of magnitudes of the growth rate, even down to a possible threshold.

In creep experiments with Wesgo Al-995 at 1100 and 1200°C it was observed that subcritical crack growth was the dominating failure mechanism [1-2]. In order to obtain a better understanding of the subcritical crack growth behaviour of Wesgo Al-995 time-to-fracture experiments were performed. In [9] the subcritical crack growth measurements at room temperature were reported. The present report describes a preliminary investigation into the subcritical crack growth behaviour of Wesgo Al-995 at 1000°C in a laboratory environment.

## 2. EXPERIMENTAL PROCEDURE

### 2.1. Material

A commercially available alumina (Wesgo Al-995) is used for the investigation. The alumina content is 99.5%, the density is  $3.85 \text{ kg/dm}^3$  and the mean grain size is  $50 \text{ }\mu\text{m}$ . In fig. 2.1 the microstructure of the material is shown, which reveals a lot of pores in the grains and at the grain boundaries. For the preparation of the bending bars, as-sintered bricks were used ( $300 \times 100 \times 50 \text{ mm}$ ). The bricks were cut into sheets, which were subsequently cut into bars of  $3.5 \times 4.5 \times 50 \text{ mm}$ . The corners of the bars were chamfered  $0.1 \text{ mm}$  at  $45^\circ$ . The four point bending characteristic strength and Weibull modulus of the material are  $270 \text{ MPa}$  and  $21.9$  at room temperature and  $184 \text{ MPa}$  and  $19.1$  at  $1000^\circ\text{C}$ . The fracture toughness  $KI_c$  is  $3.8 \text{ MPa}\sqrt{\text{m}}$  [4].

### 2.2. Time-to-fracture measurements

The bending bars were loaded with a dead-weight in four point bending at elevated temperatures in air. The temperatures of the furnace and the specimen were controlled with a master slave arrangement. The experimental set-up is shown in figure 2.2. The high temperature bending fixture has been made of SiC and was specially designed to minimise the misalignment in the load train. The support rollers of the bending fixture are at a distance of  $40 \text{ mm}$  and the inner loading span is  $20 \text{ mm}$ . For the deflection measurement of the specimen between the inner rollers, a special device similar to an arrangement developed by Fett et al. [3] was used. The displacement of the specimens were transmitted by a system of three alumina rods on a balance. The deflection in the middle of the inner span was measured with a displacement transducer. With this arrangement only the deflection caused by a constant bending moment is measured, independent of the expansion differences in the system, settlement of the support and roller flattening. The time-to-fracture, the deflection, the load and the temperature were recorded on-line by means of an A/D data-acquisition system. A detailed description of the apparatus is

given in [5], together with an evaluation of the reproducibility and accuracy of the temperature and the outer fibre bending stress during the experiments.

Before starting the time-to-fracture experiments the master thermocouples were calibrated with a certified S-type (Pt/Pt10%Rh) Rössel thermocouple. This procedure was repeated after about 1000 hours of application.

### 3. RESULTS AND DISCUSSION

For this investigation 44 time-to-fracture experiments in a laboratory environment ( $T =$  ca.  $24^{\circ}\text{C}$ ,  $\text{RH} =$  ca.  $40\%$ ) were performed. Initially a stress level of  $85\text{ MPa}$  was chosen based on a global approximation of subcritical crack growth parameters of alumina. On this stress level 10 tests were run and times-to-fracture upto 115 hours were obtained. At the higher stress levels of  $100$  and  $115\text{ MPa}$  also 10 tests were run. In table 3.1 the details of the time-to-fracture experiments are listed.

The subcritical crack growth of ceramic materials is governed by the stress intensity  $K_I$  at the crack tip:

$$K_I = \sigma \sqrt{a} Y \quad (3.1)$$

with  $\sigma =$  nominal stress

$a =$  crack length

$Y =$  geometrical factor.

The crack growth rate  $v$

$$v = da/dt \quad (3.2)$$

is usually described by a power law relation of the stress intensity

$$v = A.K_I^n = A'.(K_I/K_{Ic})^n \quad (3.3)$$

with  $A, n =$  temperature dependent material constants

$K_{Ic} =$  critical stress intensity or fracture toughness.

For ceramics the exponent  $n$  is usually higher than 15.

The time-to-fracture  $t_f$  is the time till the critical stress intensity  $K_{Ic}$  is reached. The time-to-fracture can be determined from (3.1) and (3.3) under the condition of sufficient crack growth

$$t_f = \int_{a_i}^{a_f} \frac{da}{V} = \int_{a_i}^{a_f} \frac{da}{A(\sigma \cdot Y \cdot \sqrt{a})^n} \quad (3.4)$$

Under constant load conditions equation (3.4) can be solved

$$t_f = B \cdot \sigma^{-n} \cdot \sigma_c^{n-2} \quad (3.5)$$

with  $\sigma_c$  = critical stress at the initial crack length.

The constants A, B and n can be determined from time-to-fracture test data. For the determination of the subcritical crack growth parameters from the time-to-fracture data the modified lifetime method is used [7].

By combining (3.1) and (3.2) the general equation for the time derivative can be obtained

$$dt = \frac{2}{y^2 \cdot \sigma^2 \cdot v} K_I dK_I \quad (3.6)$$

Integration from the initial crack length  $a_i$  where  $K = K_{Ii}$  to the final critical crack length  $a_c$  where  $K = K_{Ic}$  gives the time-to-fracture

$$t_f = \frac{2}{\sigma^2 \cdot y^2} \int_{K_{Ii}}^{K_{Ic}} \frac{1}{v} K_I dK_I \quad (3.7)$$

Differentiation of equation (3.6) with respect to the initial stress intensity factor and using  $K_{Ii}/K_{Ic} = \sigma/\sigma_c$  results in

$$v(K_{Ii}) = - \frac{2K_{Ic}^2}{t_f \cdot \sigma_i \cdot y^2} \frac{d[\log \sigma / \sigma_c]}{d[\log(t_f \sigma^2)]} \quad (3.8)$$

In the derivation, no special type of crack growth law is prescribed.

In alumina the initial crack size and the initial stress intensity can usually not be identified after a time-to-fracture test. For the determination of the initial stress intensity an indirect

procedure is followed, making use of the scatter of the natural cracks and the inherent scatter in the inert bending stress  $\sigma_{ci}$ . These are related by equation (3.1).

In the procedure of evaluating  $v(K_{fi})$  the Weibull data of the bending tests at high stress rates at 1000°C were used [6]. The results of the time-to-fracture tests were ranked in ascending order and analysed with the Weibull statistical distribution (see fig. 3.1 to 3.3). The  $i$ -th value of the time-to-fracture is associated with the corresponding value of the inert bending stress  $\sigma_{ci}$ , determined with the Weibull data. For the determination of the derivative part in equation (3.8) the values  $\sigma/\sigma_{ci}$  and  $t_{fi}\sigma^2$  are plotted in a log-log graph. (see fig. 3.4 to 3.6). The slope of the least squares fit through the data points is equal to the derivative part in (3.8).

For the calculation of the crack growth rate  $v$  the geometrical factor  $Y$  for natural cracks has to be known. The assumed shape of the crack is a semicircular surface flaw of length  $a$  where  $Y = 2.24/\sqrt{\pi}$  [8]. The crack growth rates for the individual time-to-fracture tests can now be calculated from (3.8). The results are plotted in fig. 3.7 to 3.9 together with the least squares fit through the data points. Fig. 3.8 shows that the crack growth data points have a rather small scatter band ( $R$  squared = 0.91) from the fit line, which means that the data can well be described by the simple power law (3.3). Within the experimental conditions there is no indication of a threshold at the lower end of the curve.

The exponent  $n$  and the constant  $A^*$  can be calculated from the slope and the intercept at  $K = K_{Ic}$  and from these data the related parameters  $A$  and  $B$ :

85 Mpa	$n = 14$	$A^* = 4.22E-4$ m/s	$A = 3.2E-12$	$B = 5155$ MPa <sup>2</sup> s
100 MPa	$n = 23$	$A^* = 1.37E-2$ m/s	$A = 5.9E-16$	$B = 63$ MPa <sup>2</sup> s
115 MPA	$n = 29$	$A^* = 4.28E-2$ m/s	$A = 4.8E-19$	$B = 15$ MPa <sup>2</sup> s

The crack growth rate data of the three series can also be plotted in one figure (fig. 3.10). This figure shows that the data points of the individual series are not in line and do not overlap. In principle the crack growth rates for a larger  $K$  range can be obtained if the

data points show the same trend. Then all the data points can also be analyzed in one fit.

The fit yields an exponent  $n = 10$  and a constant  $A^* = 1.36E-5$  m/s. With this result the other subcritical crack growth parameters can be calculated yielding the constant  $A = 1.5 E-11$  and constant  $B = 1.6E+5$  MPa<sup>2</sup>s. This result differs too much from the individual series to be valid.

In order to obtain an impression of the failure mechanism of the creep experiments on the Wesgo-Al995 material [1], the time to failure of the specimens can be plotted against the outer fibre stress in a log-log plot. If creep is the dominating failure mechanism, the slope of this plot must obey to the creep laws. In this analysis the Monkman-Grant law and the Norton power law are used resulting in [1]:

$$\sigma = c_c t_f^{-1/n_c} \quad (3.9)$$

Usually a creep exponent  $n$  between 1 and 3 is found in creep experiments with ceramics. The slope of the log  $t_f$  versus log  $\sigma$  must be in this way close to  $-1/2$ .

On the other hand if subcritical crack growth is the dominating mechanism relation (3.5) can be found.

$$\sigma = c_s t_f^{-1/n_s} \quad (3.10)$$

For subcritical crack growth the exponent  $n_s$  is about 20, so the two failure mechanisms can be distinguished in a log  $t_f$  -log  $\sigma$  plot. Generally such a plot has the characteristics of figure 3.11. In the higher stress regions subcritical crack growth is the mayor mechanism with a small negative slope, while in the lower stress region creep dominates with a much steeper line. In practice subcritical crack growth did not show a straight line in the log-log plot due to deviations from the power law and the stress redistribution in the beginning of the bending experiment at high temperature, but the slope of a line through the data points gives a good indication of the mechanism involved.

In figure 3.12 the times to failure are plotted against the outer fibre stress for the experiments at 1100°C. In this figure slopes of  $-1/20$  and  $-1/2$  are indicated. The data points are close to a line which is not so steep, indicating that the failure mechanism of the creep experiments described in [1] is subcritical crack growth. The irregular and inconsistent creep curves are obviously due to this failure mechanism.

#### 4. CONCLUSIONS AND RECOMMENDATIONS

The Wesgo Al 995 alumina is susceptible to subcritical crack growth at high temperatures in air.

In creep experiments with this material subcritical crack growth is the dominating failure mechanism in the experimental conditions used in the investigation. This leads to irregular and inconstant creep curves.

The subcritical crack growth parameters of Wesgo Al-995 alumina are determined with the modified lifetime method. The parameters for a stress of 100 MPa are:

$$v = A^* \cdot (K_I/K_{Ic})^n \qquad A^* = 0.0137 \text{ m/s}$$

$$n = 23$$

$$t_f = B \cdot \sigma^{-n} \cdot \sigma_c^{n-2} \qquad B = 62.9 \text{ MPa}^2\text{s}$$

$$n = 23$$

The crack growth data points have a rather small scatter band from the fit line, which means that the data can be described by the simple power law.

Within the experimental conditions there is no indication of a threshold at the lower end of the curve.

It is recommended to repeat these experiments with a larger series of specimens (at least 20) and at several temperatures (600-1200°C) in order to obtain a better determination of the subcritical crack growth parameters of Wesgo Al-995 alumina.

## 5. ACKNOWLEDGMENTS

The author likes to thank Mr. N.P.G. van der Burg for performing the time-to-fracture experiments.

## 6. REFERENCES

- [1] Bach, P.W., Creep Experiments on Wesgo Al-995, ECN-C--91-070.
- [2] Bach, P.W., de Smet, B.J., Creep Experiments on Alumina, Proc. ECerS, Augsburg, 1991.
- [3] Fett, T., Keller, K. and Munz, D., An Analysis of the Creep of Hot Pressed Silicon Nitride in Bending. J. Mater.Sci. 23, 1988, 467-474.
- [4] De Smet, B.J., Bach, P.W., Scholten, H.F., Dortmans, L.J.G.M. and De With, G., Weakest-Link Failure Predictions for Ceramics III: Uniaxial and Biaxial Bending Tests on Alumina, to be published in J.Eur.Cer.S.
- [5] Van der Burg, N.P.G. and Bach, P.W., Evaluatie van de opstelling voor kruipproeven onder vierpunts buigbelasting, ECN-I--91-013.
- [6] De Smet, B.J., Bending Strength of Alumina at High Temperatures, ECN-C--92-005.
- [7] Fett, T., Munz, D., Evaluation of Subcritical Extension under Constant Loading, J.Eur.Cer.Soc. 6, 1990, 67-72.
- [8] Trantina, G.G., Fracture Mechanics Analysis of Defect Sizes, in Methods for Assessing the Structural Reliability of Brittle Materials, ASTM STP 844, 1984, 117-130.
- [9] Bach, P.W. and De Smet, B.J., Subcritical Crack Growth of Wesgo Al-995 Alumina at Room Temperature, ECN-C--92-026.

Table 3.1. List of the time-to-fracture test results.

85 MPa tf [s]	100 MPa tf [s]	115 MPa tf [s]
1094	130	7
1400	191	15
1490	310	50
1937	360	180
2509	1890	190
2959	2091	210
4090	2930	270
8165	3841	490
8517	4417	1130
10771	5335	1861

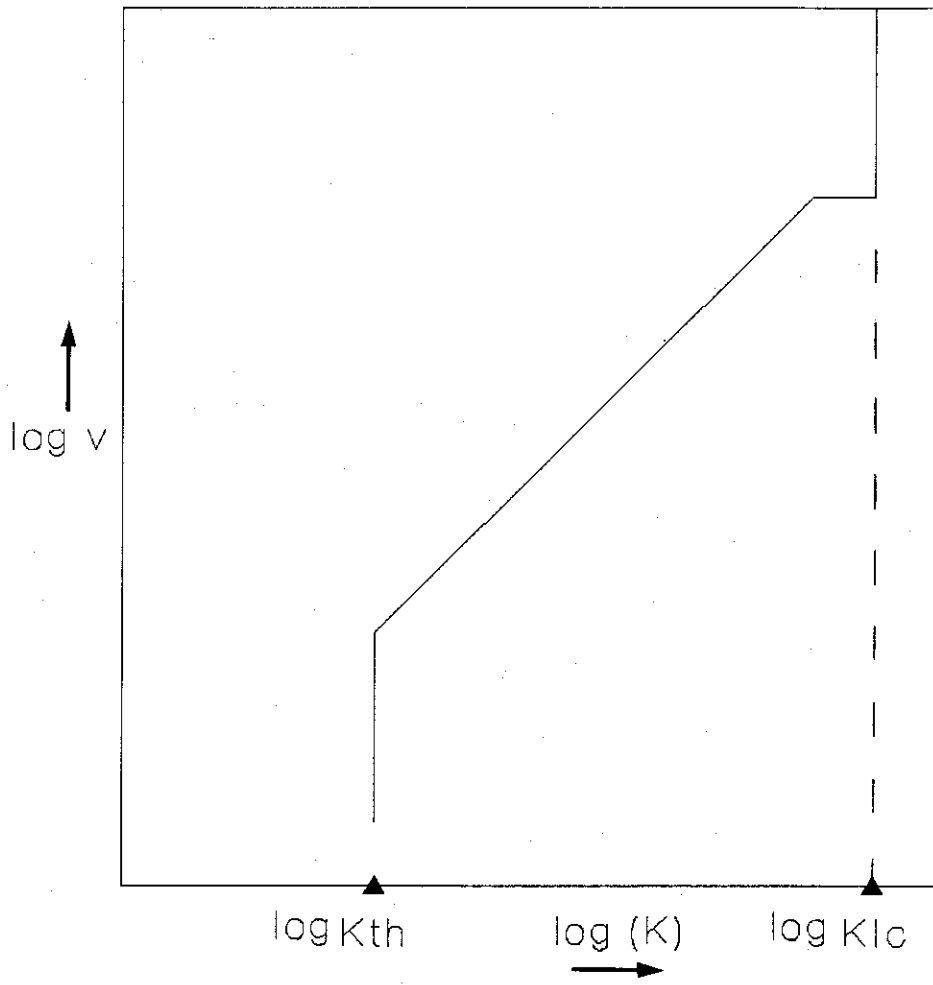


Fig. 1.1. Typical subcritical crack growth curve.

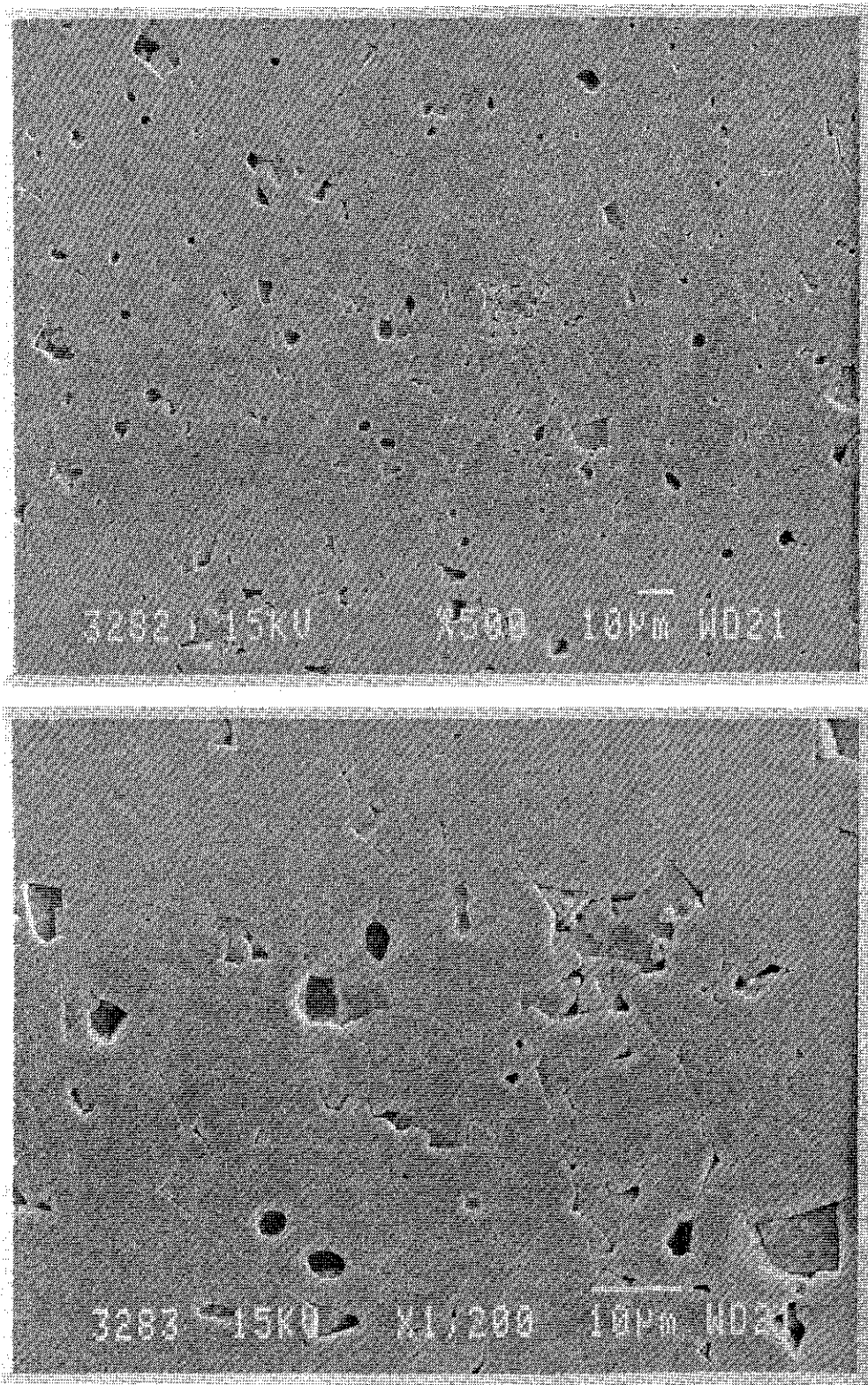


Figure 2.1. The microstructure of Wesgo Al 995.

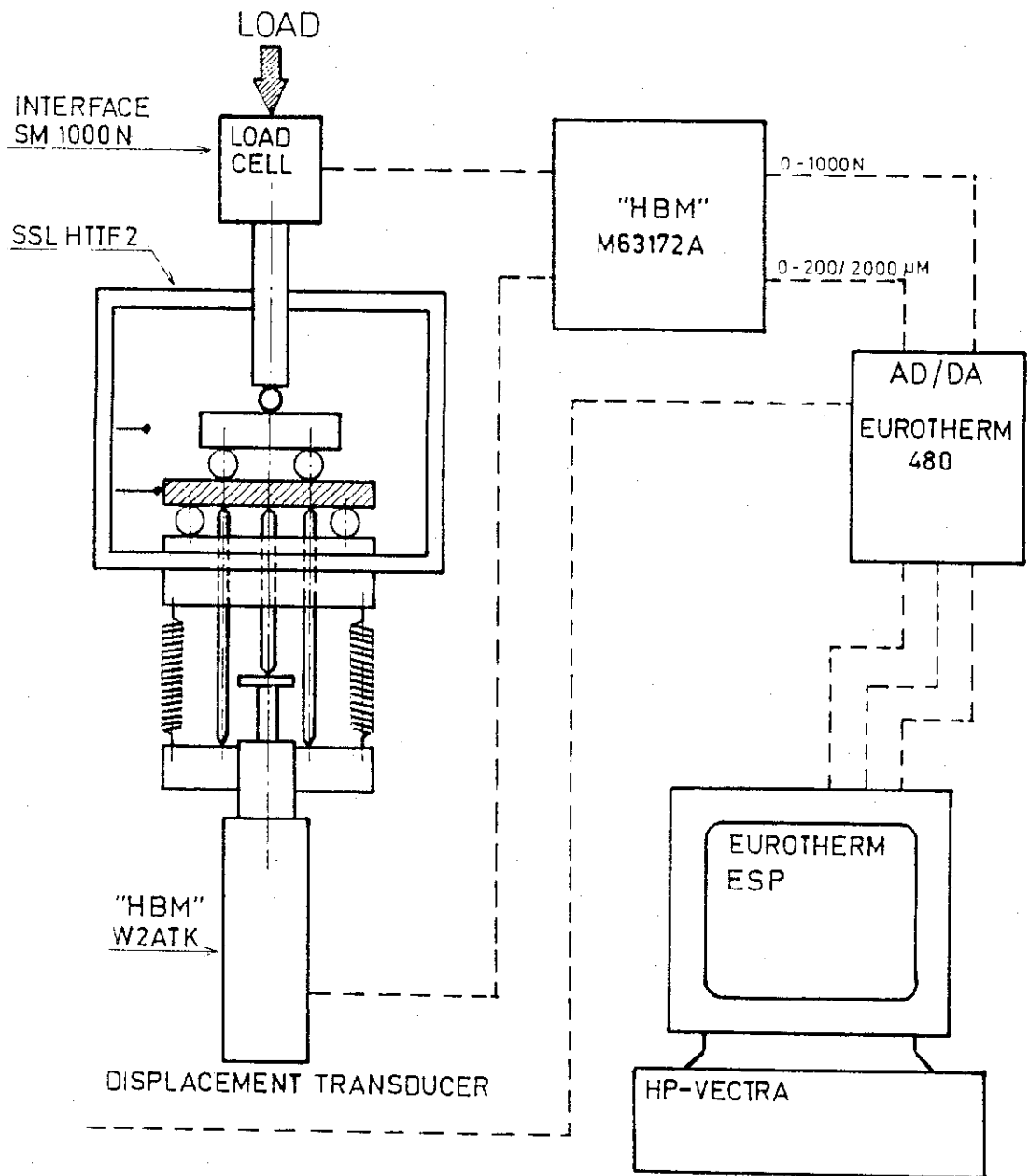


Fig. 2.2. Experimental set-up for the time-to-fracture tests.

# Subcritical Crack Growth, alumina

Temp: 1000 °C RH: 30% Sigma: 85 MPa

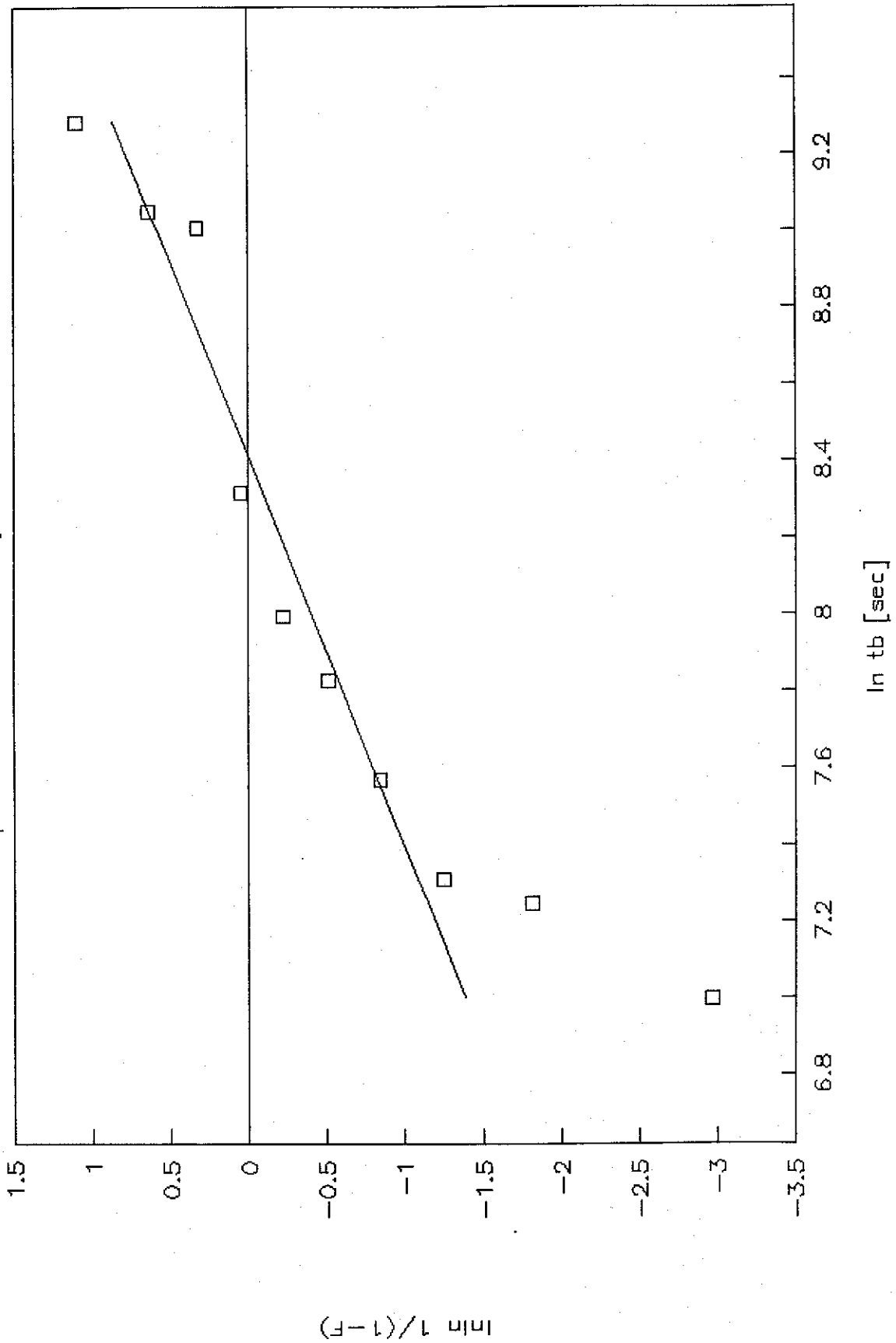


Fig. 3.1. Weibull plot of the time-to-fracture data for  $\sigma = 85$  MPa.

# Subcritical Crack Growth, alumina

Temp: 1000 °C RH: 30% Sigma: 100 MPa

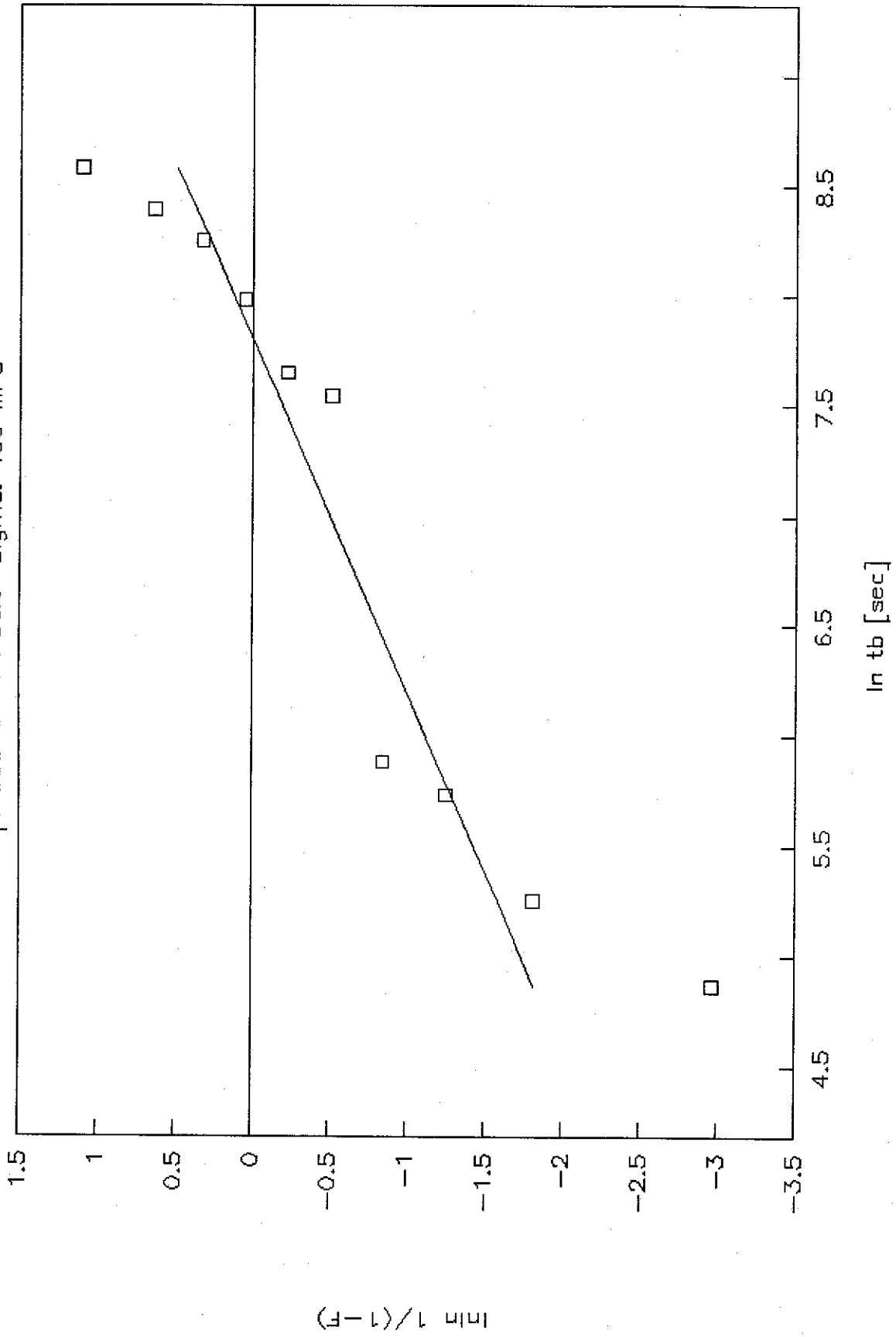


Fig. 3.2. Weibull plot of the time-to-fracture data for  $\sigma = 100$  MPa.

# Subcritical Crack Growth, alumina

Temp: 1000 °C RH: 30% Sigma: 115 MPa

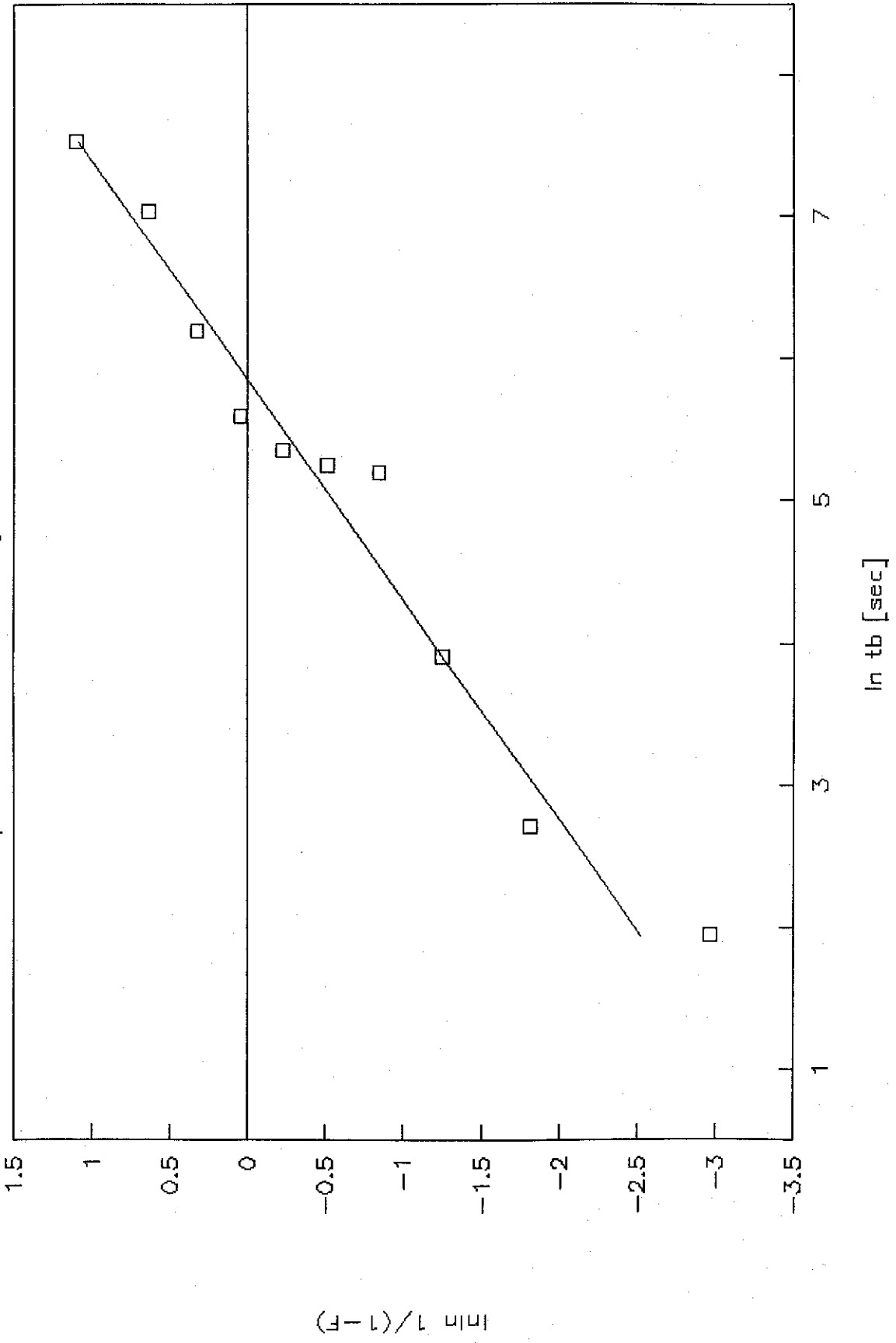


Fig. 3.3. Weibull plot of the time-to-fracture data for  $\sigma = 115$  MPa.

# Subcritical Crack Growth, alumina

Temp: 1000 °C RH: 30% Sigma: 85 MPa

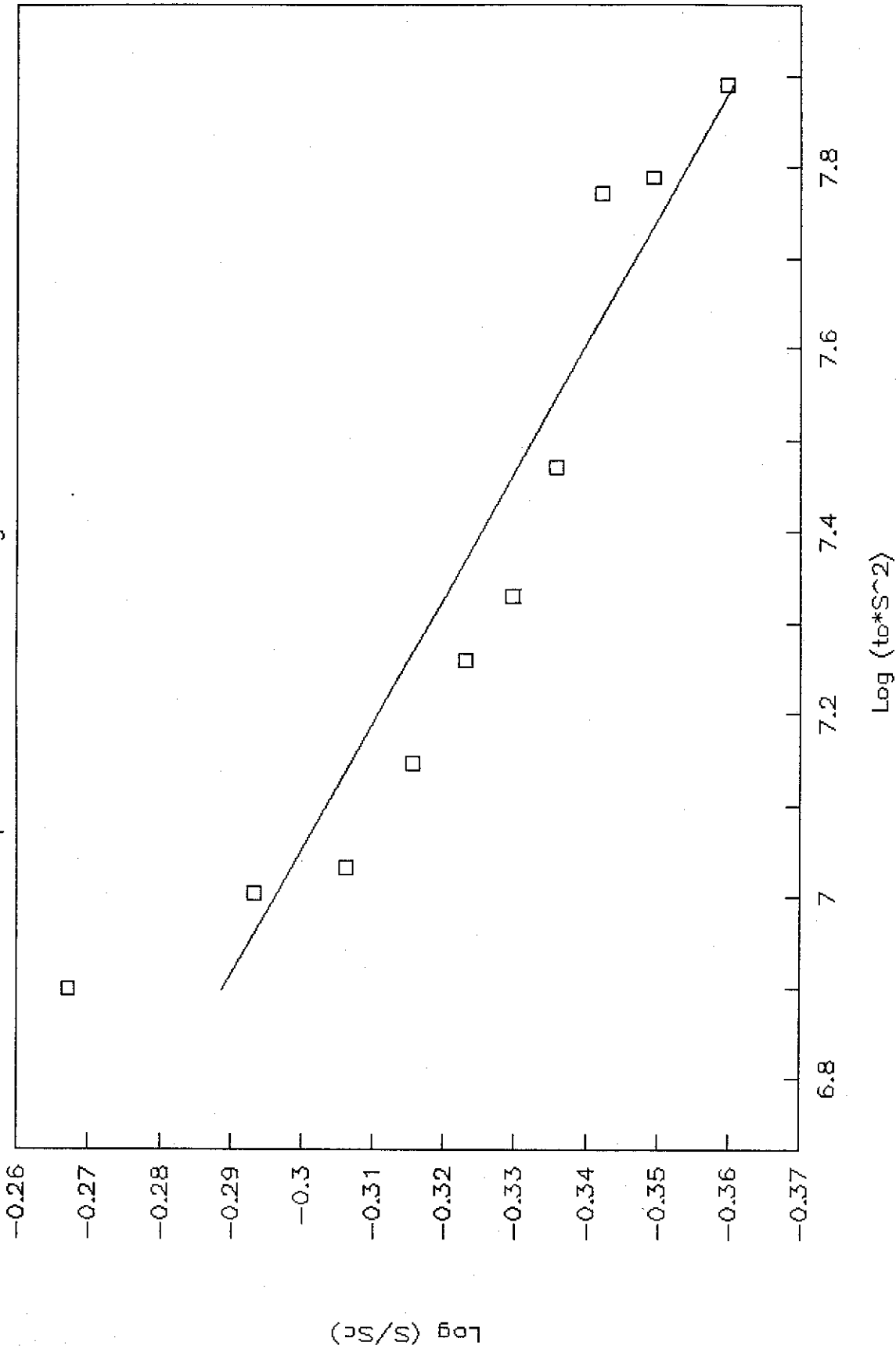


Fig. 3.4. Plot for the determination of the derivative part in the crack growth equation (3.8) for  $\sigma = 85$  MPa.

# Subcritical Crack Growth, alumina

Temp: 1000 °C RH: 30% Sigma: 100 MPa

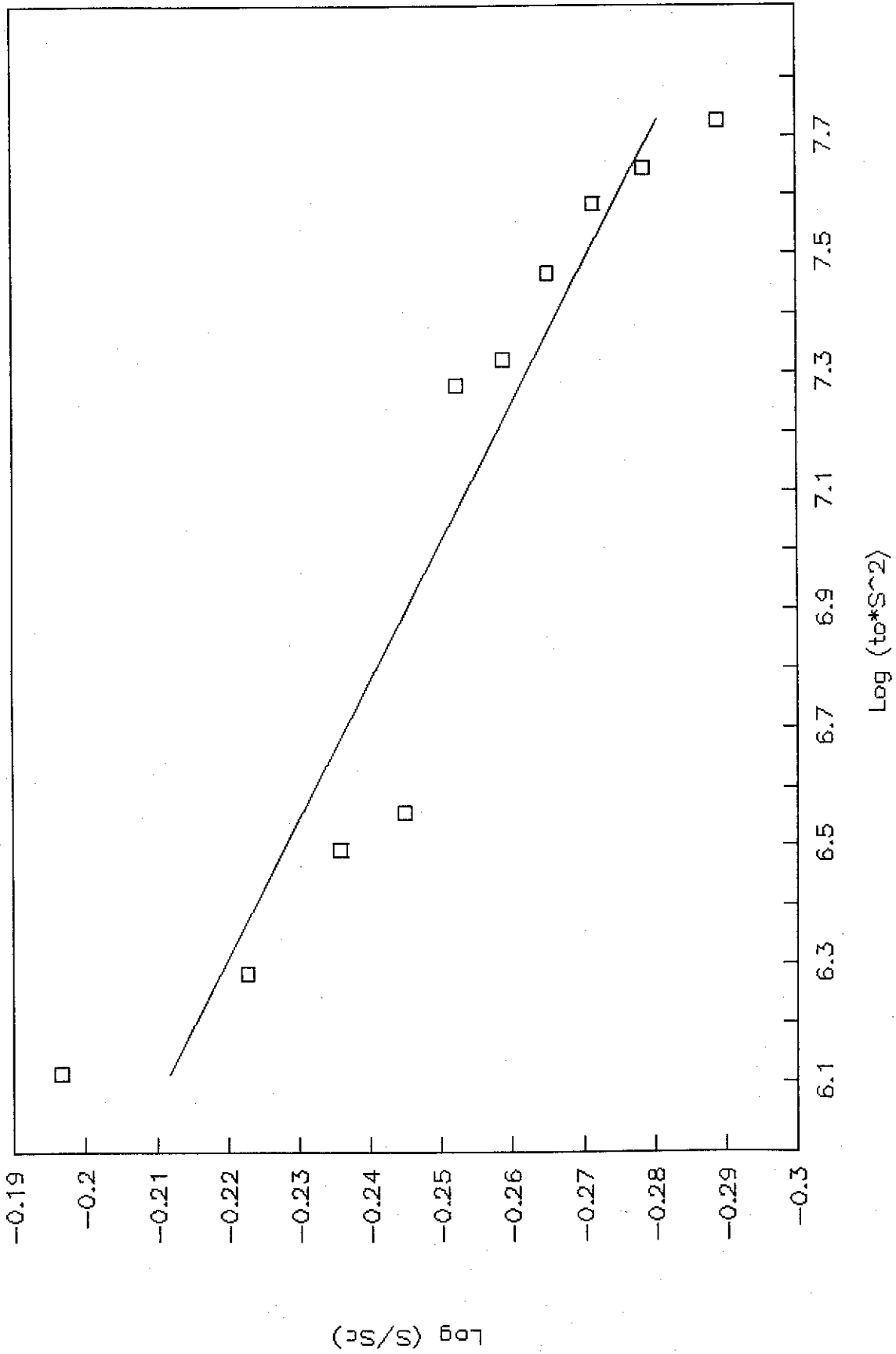
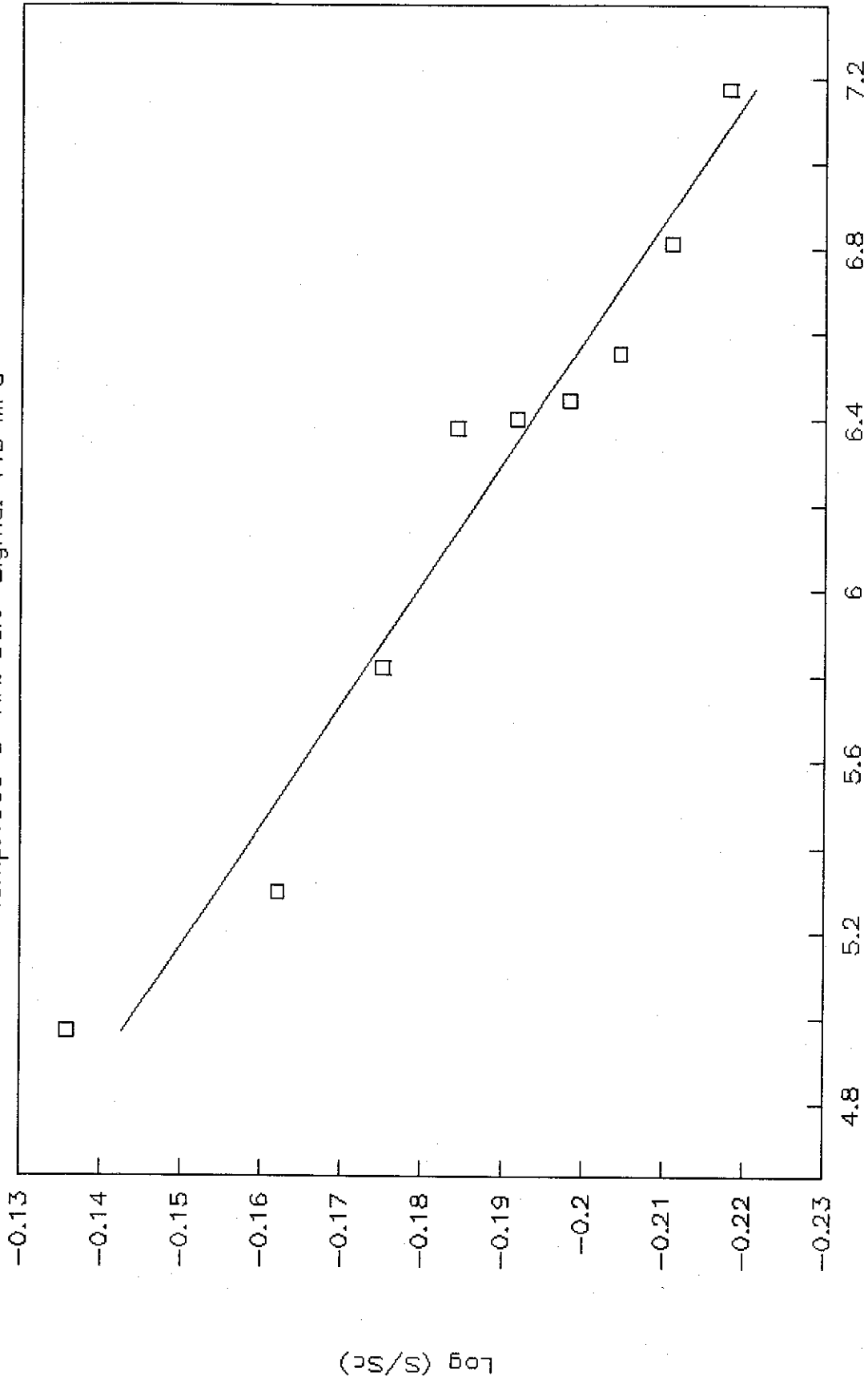


Fig. 3.5. Plot for the determination of the derivative part in the crack growth equation (3.8) for  $\sigma = 100$  MPa.

# Subcritical Crack Growth, alumina

Temp: 1000 °C RH: 30% Sigma: 115 MPa



Log (ta\*S^2)

Fig. 3.6. Plot for the determination of the derivative part in the crack growth equation (3.8) for  $\sigma = 115$  MPa.

# Subcritical Crack Growth, alumina

Temp: 1000 °C RH: 30% Sigma: 85 MPa

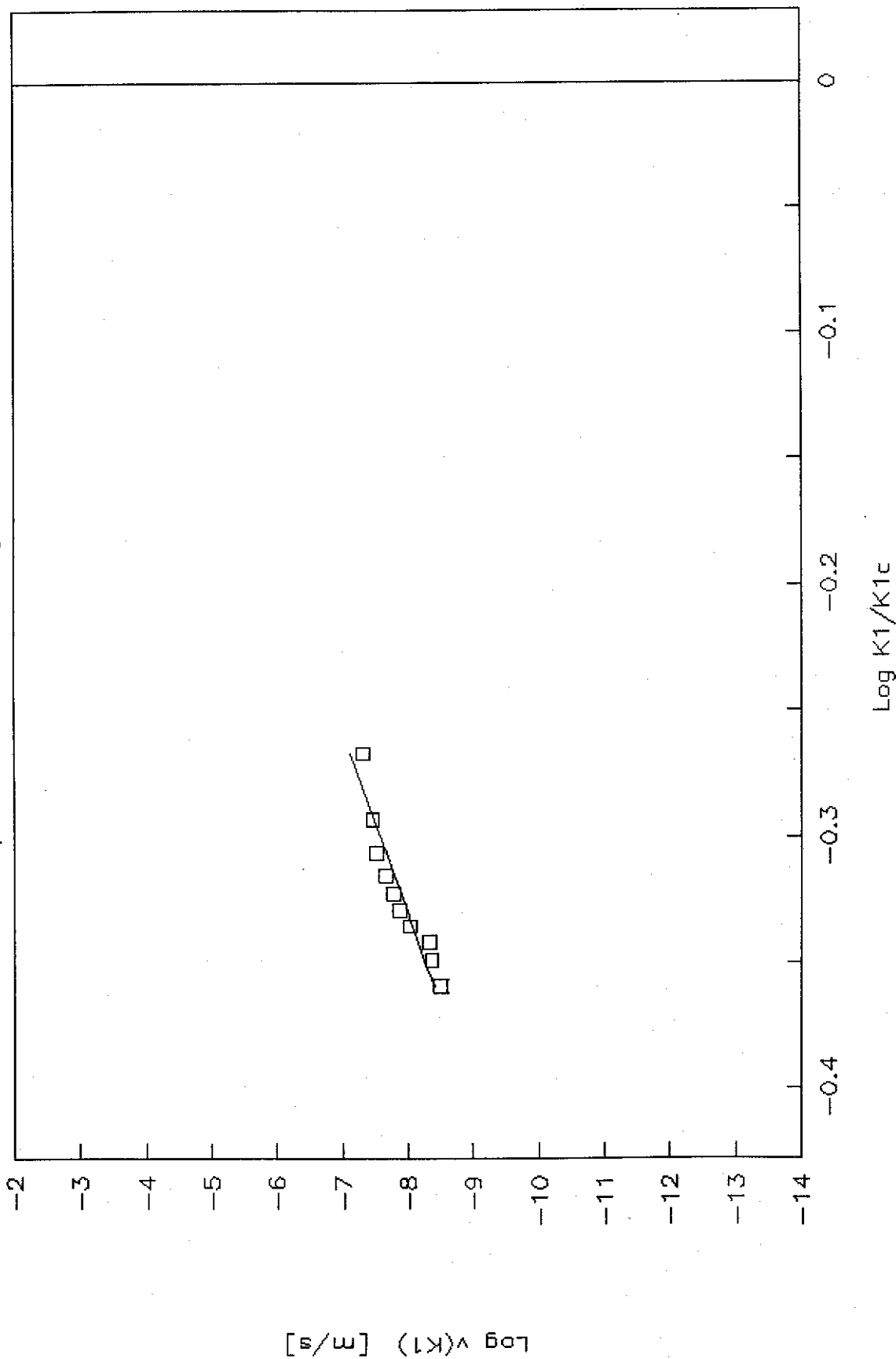


Fig. 3.7. Subcritical crack growth curve for the  $\sigma = 85$  MPa series.

# Subcritical Crack Growth, alumina

Temp: 1000 °C RH: 30% Sigma: 100 MPa

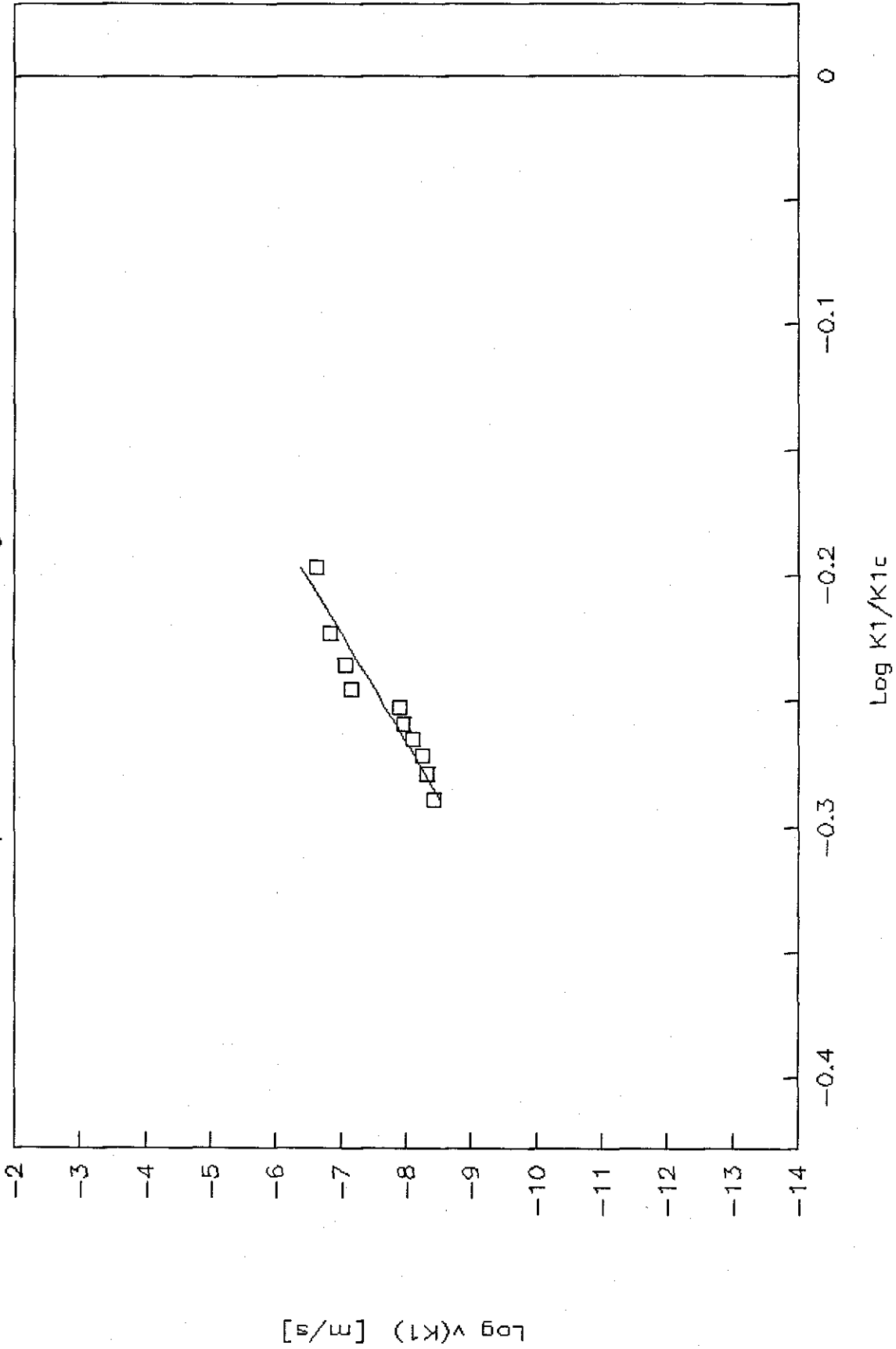


Fig. 3.8. Subcritical crack growth curve for the  $\sigma = 100$  MPa series.

# Subcritical Crack Growth, alumina

Temp: 1000 °C RH: 30% Sigma: 115 MPa

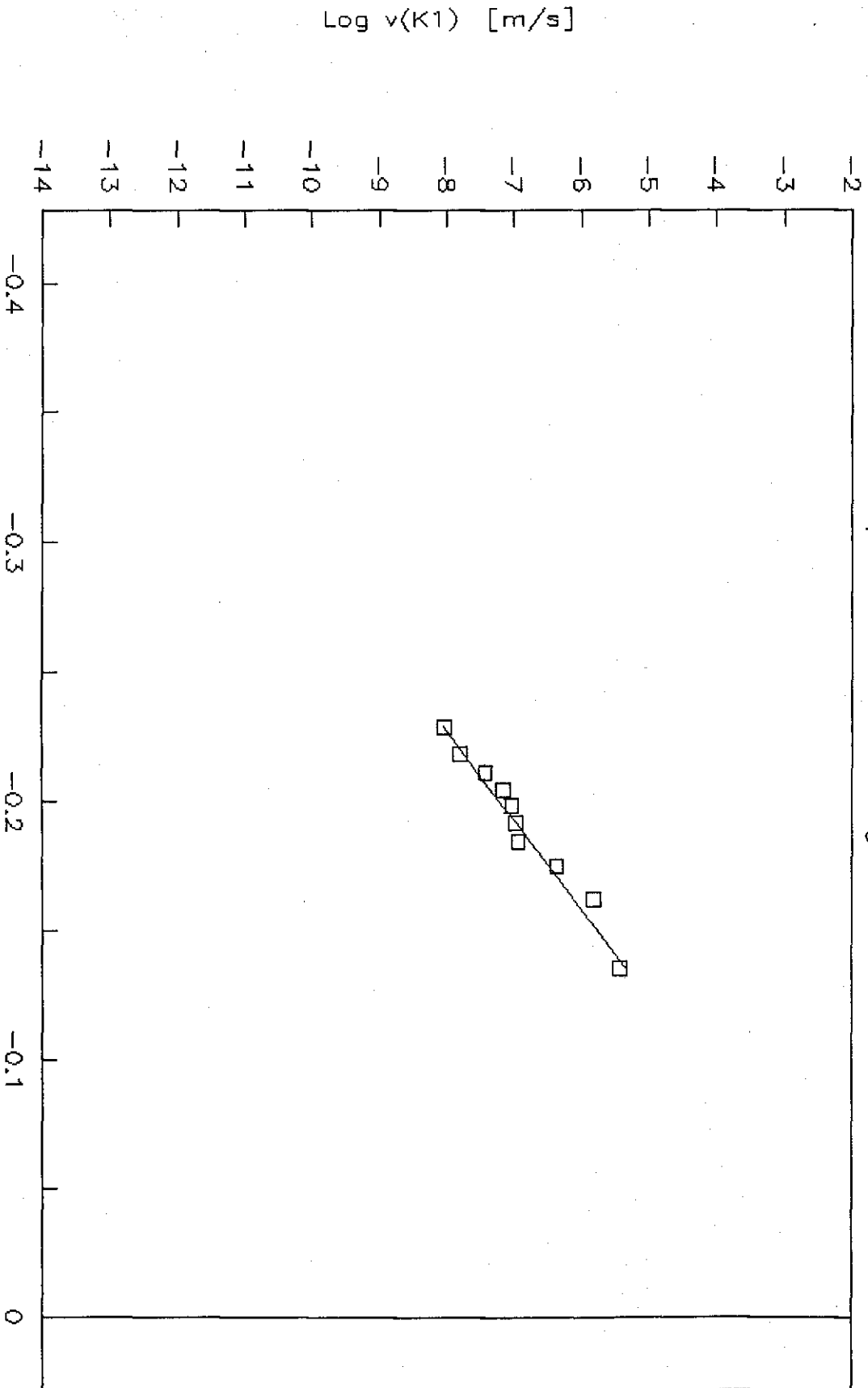


Fig. 3.9. Subcritical crack growth curve for the  $\sigma = 115$  MPa series.

# Subcritical Crack Growth , alumina

Temp: 1000 °C RH: 30%

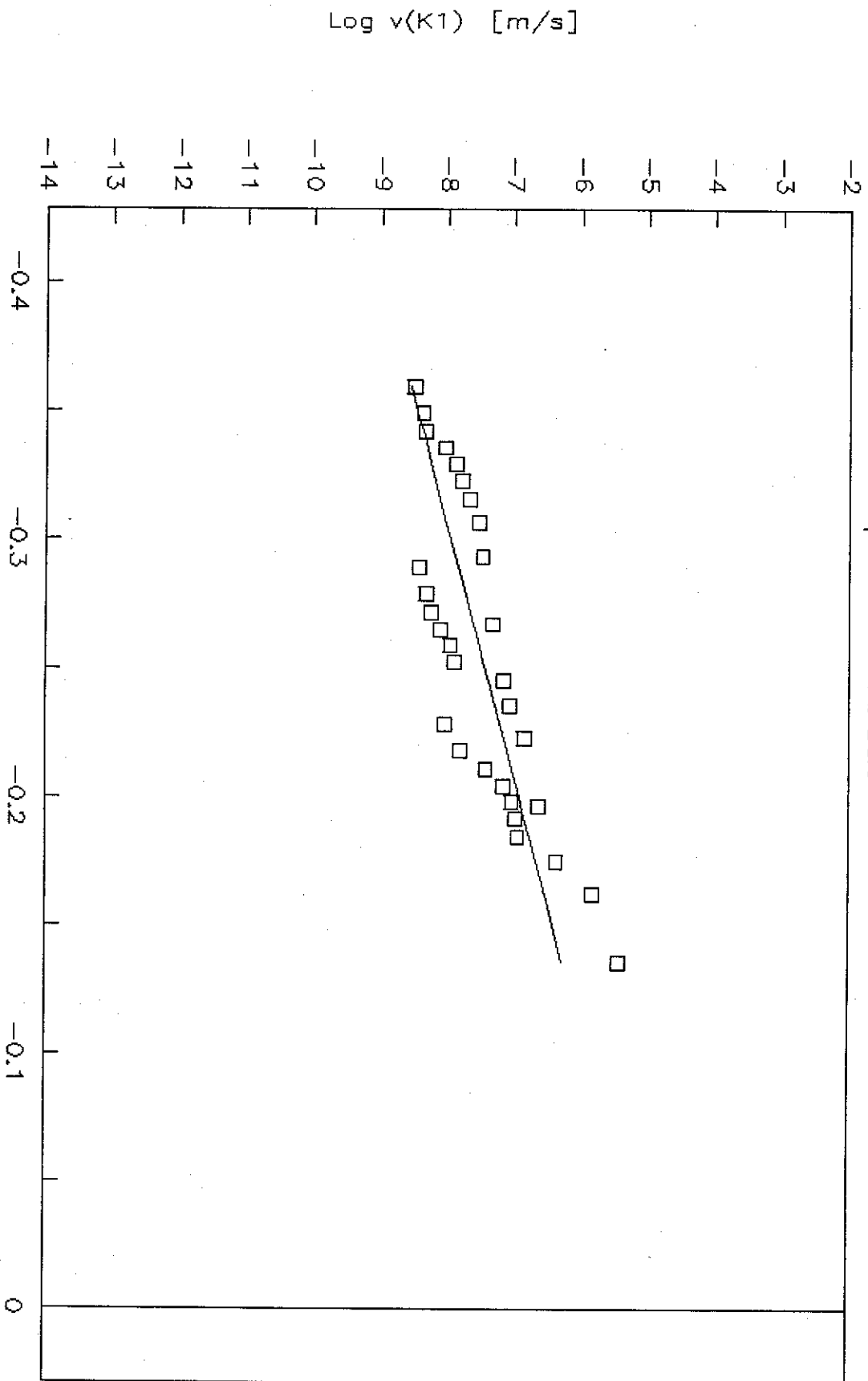


Fig. 3.10. Subcritical crack growth curve of all the data points.

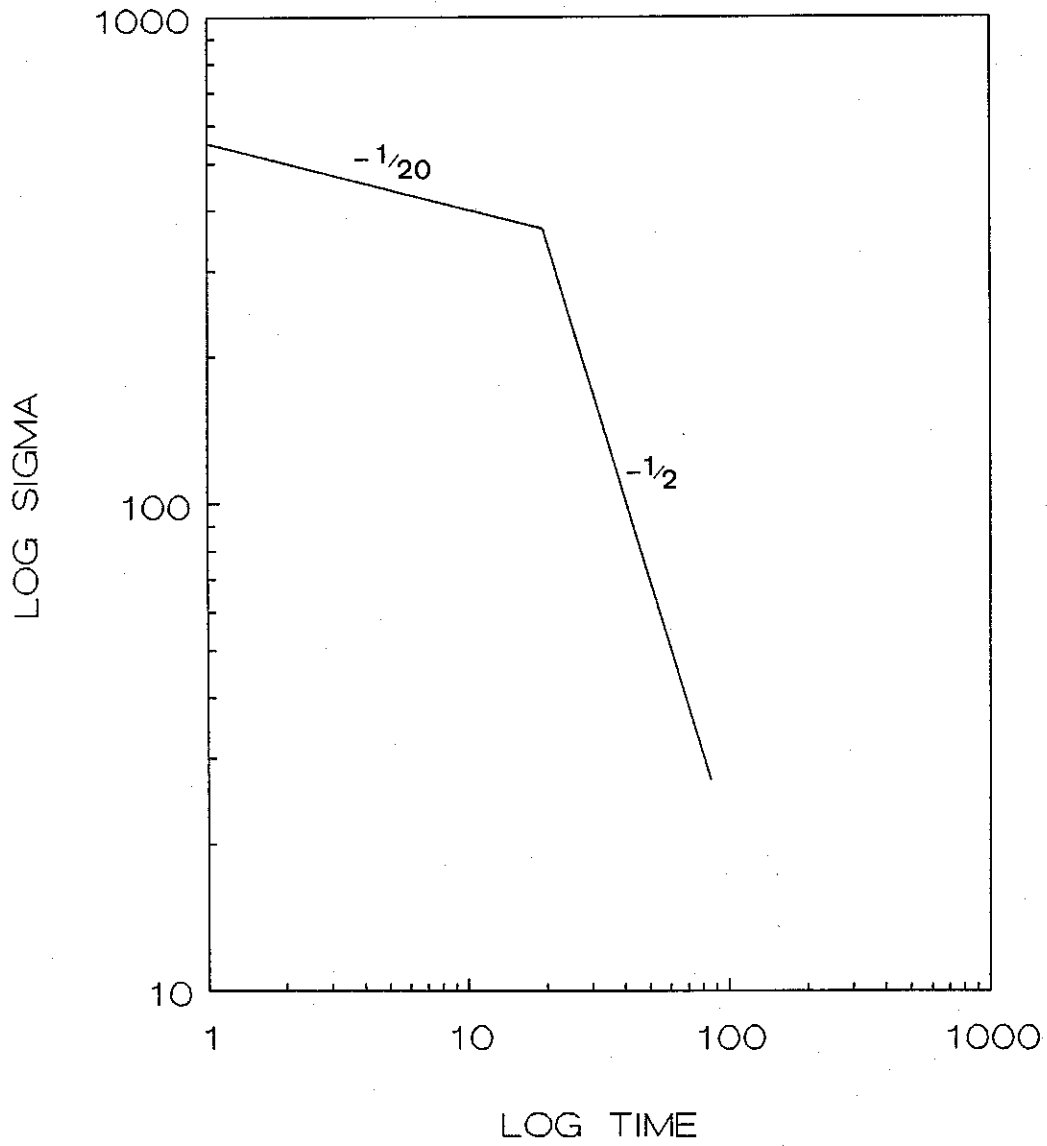


Fig. 3.11. Schematical example of a time-to-failure plot.

# WESGO

spann. vs. tijd tot breuk 1100C

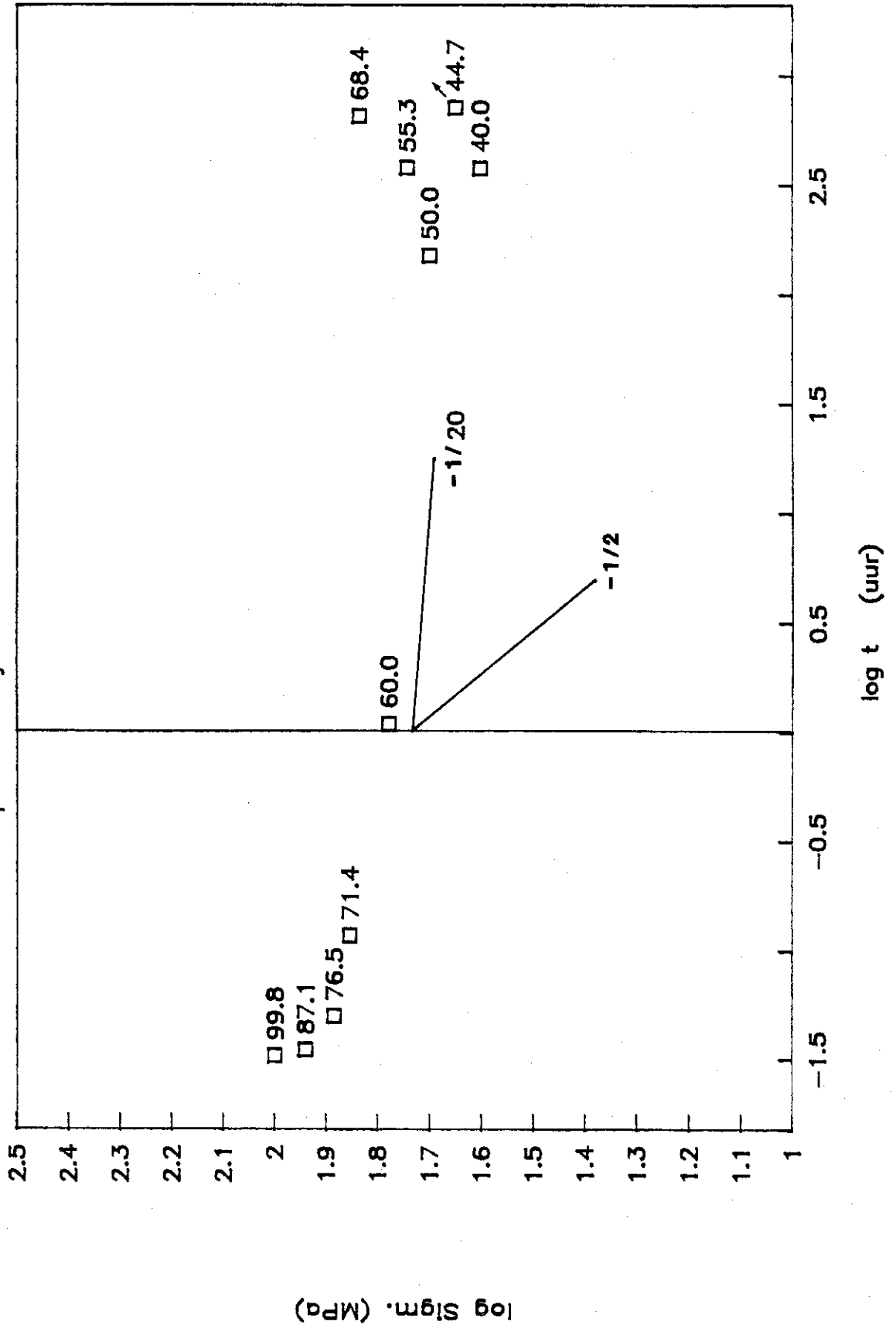


Fig. 3.12. Time-to-failure of creep experiments on Wesgo Al-995 [1].